

Article

Electrochemical Determination of Lead & Copper Ions Using Thiolated Calix[4]arene-Modified Screen-Printed Carbon Electrode

Chong Jin Mei ¹, Nor Azah Yusof ² and Shahrul Ainliah Alang Ahmad ^{1,2,*}

¹ Department of Chemistry, Faculty of Science, Universiti Putra Malaysia, 43400 Serdang, Malaysia; jinmei95@hotmail.com

² Institute of Advanced Technology, Universiti Putra Malaysia, 43400 Selangor, Malaysia; azahy@upm.edu.my

* Correspondence: ainliah@upm.edu.my

Abstract: This study used a thiolated calix[4]arene derivative modified on gold nanoparticles and a screen-printed carbon electrode (TC4/AuNPs/SPCE) for Pb²⁺ and Cu²⁺ determination. The surface of the modified electrode was characterised via Fourier-transform infrared spectroscopy (FTIR), field emission scanning electron microscopy (FESEM), cyclic voltammetry (CV), and electrochemical impedance spectroscopy (EIS). Differential pulse voltammetry (DPV) was used for the detection of Pb²⁺ and Cu²⁺ under optimum conditions. The limit of detection (LOD) for detecting Pb²⁺ and Cu²⁺ was 0.7982×10^{-2} ppm and 1.3358×10^{-2} ppm, respectively. Except for Zn²⁺ and Hg²⁺, the presence of competitive ions caused little effect on the current response when detecting Pb²⁺. However, all competitive ions caused a significant drop in the current response when detecting Cu²⁺, except Ca²⁺ and Mg²⁺, suggesting the sensing platform is more selective toward Pb²⁺ ions rather than copper (Cu²⁺) ions. The electrochemical sensor demonstrated good reproducibility and excellent stability with a low relative standard deviation (RSD) value in detecting lead and copper ions. Most importantly, the result obtained in the analysis of Pb²⁺ and Cu²⁺ had good recovery in river water, demonstrating the applicability of the developed sensor for real samples.

Keywords: calixarene; screen printed-carbon electrode (SPCE); differential pulse voltammetry (DPV); heavy metal; lead (Pb²⁺); copper (Cu²⁺)



Citation: Mei, C.J.; Yusof, N.A.; Alang Ahmad, S.A. Electrochemical Determination of Lead & Copper Ions Using Thiolated Calix[4]arene-Modified Screen-Printed Carbon Electrode. *Chemosensors* **2021**, *9*, 157. <https://doi.org/10.3390/chemosensors9070157>

Academic Editor: Sadanand Pandey

Received: 24 May 2021
Accepted: 16 June 2021
Published: 25 June 2021

Publisher's Note: MDPI stays neutral with regard to jurisdictional claims in published maps and institutional affiliations.



Copyright: © 2021 by the authors. Licensee MDPI, Basel, Switzerland. This article is an open access article distributed under the terms and conditions of the Creative Commons Attribution (CC BY) license (<https://creativecommons.org/licenses/by/4.0/>).

1. Introduction

Heavy metals, which have been recently termed “potentially toxic elements” [1], are a serious environmental problem that have caught global attention as they pose a great threat to life on earth [2–4]. Mining, logging, and agricultural activities are the possible causes that have increased heavy metal concentrations in rivers, resulting in polluted waters [5]. Lead (Pb) is a bluish-grey metal found in the crust of the earth. Investigations have verified that the human nervous system is the most prominent target of Pb poisoning, with symptoms such as headaches, memory loss, and lack of attention. Moreover, pregnant women who are exposed to or who consume Pb will pass Pb to the fetus, thus possibly causing premature childbirth and low weight in the fetus. Moreover, children exposed to Pb may suffer from abnormalities in brain development [6].

Copper (Cu), one of the most abundant metals and essential trace elements on earth, plays a vital role in various biological processes [7,8]. Despite being categorised as a heavy metal, Cu is essential to human health; it is permissible for adults to consume a daily intake of Cu that varies between 0.9 mg and 2.2 mg. However, Cu becomes toxic at high concentrations of above 1.3 mg L^{-1} , possibly causing changes to the nervous system, depression, lung cancer, and gastrointestinal irritation [3]. Furthermore, exposure to Cu may also lead to hypertension, lethargy, gastrointestinal bleeding, and DNA damage [9].

Considering the adverse effects caused by heavy metals, various analytical methods have been introduced to detect heavy metal ions. These methods include atomic absorption

spectrometry [10], fluorescence spectrophotometry (FL) [11], and inductively coupled plasma mass spectroscopy (ICP-MS) [12]. However, great challenges still exist, as these techniques require pre-treatment processes, a long analysis time, a qualified operator to handle the equipment, and costly instrumentation [13,14]. Electroanalytical techniques are a promising alternative for target analyte quantification [15]. Electrochemical approaches are employed to determine heavy metal ions due to their short analysis time, simplicity, low cost, sensitivity, good selectivity, portability, and enablement of in situ analysis without any sophisticated instrumentation. Besides, the method also offers ease of operation and low maintenance cost [16,17]. Due to these advantages, the electrochemical technique is deemed more beneficial for field analysis [16].

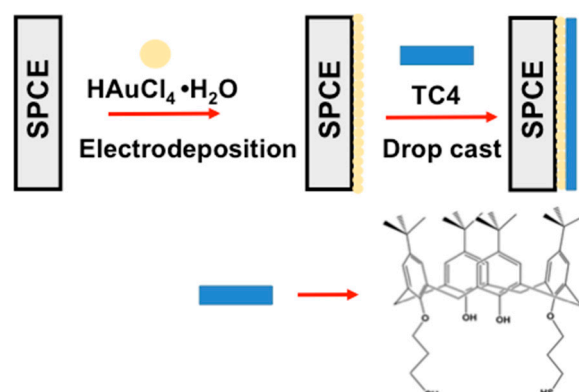
Initially, the mercury drop electrode was used for the stripping analysis in heavy metal ion tracings; however, it has been found not suitable for sensing applications due to its toxicity [18]. Carbon-based electrode materials were then introduced after several alternatives because carbon materials can improve the selectivity and sensitivity of target analytes through surface modification based on selective functionalities, i.e., potential affinity toward selective metal ions [19].

Recently, significant focus has been made to fabricate and modify single-use, disposable electrodes, such as the screen-printed electrode (SPE). This electrode has great benefits in many research areas because of its broad potential range, low sample volume (μL), low-cost production, and adaptability. Besides, this electrode can be easily modified by using different commercially available inks for working, counter, and reference electrodes [16,19].

Various materials have been used to modify the SPCE surface for the electrochemical determination of heavy metal ions, including nanomaterials [20], metal oxides [21], metal films [22], polymers [23], carbon nanotubes [24], carbon dots [25], reduced graphene oxide [26], and biomaterials [27]. Nowadays, molecular recognition of host–guest chemistry has incited great research enthusiasm [28]. Calixarenes (the host) have attracted great potential interest because they can react with guest molecules, such as cations, anions, and neutral molecules, to form stable host–guest complexes [28]. These compounds have a strong recognition ability [29], which enables them to maintain their complexation ability in a mixed monolayer [30]. Nevertheless, their non-conducting property limits their utilization in electrical devices.

Nanomaterials such as carbon-based materials, metal oxides, and gold nanoparticles (AuNPs) possess high electroactive surface areas that are able to improve sensing performance by facilitating electron transfer between surface electrodes and analytes [31,32]. Specifically, AuNPs have attractive optical, electronic, catalytic, and thermal properties [33] and gained great interest in various fields, including chemistry, physics, biology, material sciences, medicine, and other interdisciplinary fields, due to their potential applications. Our previous work has shown that integration of a nanomaterial, which in this case was reduced graphene oxide (rGO), into calixarene derivatives enhanced the conductivity of the host, leading to low detection limit of analytes [34].

In the present work, AuNPs were used due to their promising properties in enhancing sensor performance. Thiolated calixarene derivatives with short alkanethiol spacers (two C_3) were used as a host for target molecule sensing and the chemisorption of thiolated calix[4]arene on AuNPs modified on a screen-printed carbon electrode (SPCE) (as shown in Scheme 1) enabled us to produce a compact layer and improve the conductivity in the analytical measurement of Pb^{2+} and Cu^{2+} using differential pulse voltammetry (DPV). The modified electrode was then applied in real sample analysis.



Scheme 1. The electrode modification pathway for the electrochemical determination of Pb^{2+} and Cu^{2+} .

2. Materials and Methods

Gold (III) chloride hydrate was purchased from Sigma-Aldrich (St. Louis, MI, USA). Potassium chloride (KCl), chloroform (CHCl_3), and copper (II) sulphate were purchased from R&M Chemicals (Petaling Jaya, Malaysia). Phosphate buffer saline (PBS) solution and potassium ferrocyanides ($\text{K}_4[\text{Fe}(\text{CN})_6]$) were purchased from Bendosen (Kuala Lumpur, Malaysia). Standard lead solution (1000 ppm) was purchased from Merck (Kenilworth, NJ, USA). Deionised water (18.2 M Ω) was used throughout the experiments. Thiolated calix[4]arene (TC4) was synthesised and obtained from Dr. Irene Ling (Monash University Malaysia). Screen-printed carbon electrodes (C110) with a 4 mm diameter were purchased from Metrohm Malaysia Sdn Bhd, consisting of working and counter electrodes from carbon-based material and a reference electrode from silver-based material.

Measurements of pH were performed using a FiveEasy pH meter F20 from Mettler Toledo (Columbus, OH, USA). Chronoamperometry (CA), cyclic voltammetry (CV), and differential pulse voltammetry (DPV) were performed using an AUTOLAB instrument Model uAutolab Type III (Eco Chemie B.V., Utrecht, The Netherlands) followed by data analysis using Nova 1.11 software. Electrochemical impedance spectroscopy (EIS) measurements were taken using an AUTOLAB PGSTAT204 potentiostat model connected to an FRA impedance potentiometric FRA32M module. The Fourier-transform infrared (FTIR) spectra were analysed using a Thermo Scientific Nicolet 6700 FT-IR spectrometer (Thermo Scientific, MA, USA) from 400 cm^{-1} to 4000 cm^{-1} using the attenuated total reflection (ATR) method. Field emission scanning electron microscopy (FESEM) images and energy dispersive X-ray (EDX) graphs were obtained using a FEI Nova Nanosem 230 instrument (FEI, Eindhoven, Holland). Inductively coupled plasma data were collected using a PerkinElmer Optima 2000 DV (PerkinElmer, Shelton, MA, USA).

2.1. Surface Modification of Screen-Printed Carbon Electrode

2.1.1. Electrodeposition of AuNPs on SPCE(AuNPs/SPCE)

Gold nanoparticles (AuNPs) were electrodeposited on a screen-printed carbon electrode using a previous method [35]. Gold (III) chloride hydrate (HAuCl_4) salt was dissolved in deionised water to form a 2 mM gold–salt solution. The solution was then electrodeposited onto the working electrode surface via chronoamperometry, with an applied potential of -0.3 V, at 300 s. The AuNPs/SPCE was then washed carefully with deionised water and left to dry at room temperature. AuNPs/SPCE was then electrochemically activated in 0.1 M PBS using cyclic voltammetry (CV) by scanning from 0.8 V to 1.3 V for 5 cycles with a scan rate of 100 mV/s. Finally, the AuNPs/SPCE was washed carefully with deionised water and left to dry at room temperature prior to use.

2.1.2. Modification of AuNPs/SPCE with TC4

The surface of the AuNPs/SPCE was further modified with TC4 by drop-casting 2 μL of 0.2 g/L of TC4 dissolved in chloroform on the AuNPs/SPCE for 3 h. The modified electrode was left to dry at room temperature in a desiccator prior to detection.

2.2. Electrochemical Analysis of Analytes

The analytical performance of the analytes was studied using CV, DPV, and EIS. CV was performed by immersing the electrode in 0.1 M KCl containing 1 mM of $\text{K}_3[\text{Fe}(\text{CN})_6]$ solution within the range -0.5 V to 0.5 V with a scan rate of 100 mV/s for 10 cycles. Meanwhile, EIS analysis was performed in the same solution from 100 kHz to 0.1 Hz, 10 per decade, and at 0.005 V amplitude. DPV was used to analyse 1 ppm Pb^{2+} in 0.1 M KCl at a potential of -1.2 V (Pb^{2+}) and -1.1 V (Cu^{2+}), a deposition time of 120 s, and a scan rate of 100 mV/s.

Recovery Study

The recovery study was conducted using electrochemical and ICP-OES techniques. In the electrochemical technique, the collected samples were first purified via filtration to eliminate solid impurities or suspended particulate matter. Subsequently, 2.5 mL of this solution was added to 2.5 mL of 0.1 M KCl solution. The recovery measurement was taken by spiking Pb^{2+} and Cu^{2+} solutions, respectively, into the mixture solution without further treatment.

In the ICP-OES technique, standard solutions were prepared for instrument calibration. For sample preparation, 20 mL of sample was first filtered by a cellulose nitrate membrane filter, 0.45 μm , followed by spiking Pb^{2+} and Cu^{2+} solutions, respectively, into the samples. The samples were analysed, and the data directly showed the concentration value of Pb^{2+} and Cu^{2+} presence in the samples.

3. Results and Discussion

3.1. Characterisations of Modified Electrodes

3.1.1. Fourier-Transform Infrared Spectroscopy

Fourier-transform infrared spectroscopy was used to verify the modification of the thiolated calix[4]arene (TC4) on the AuNPs/SPCE surface. As shown in Figure 1, the FTIR spectra of both the bare SPCE and the AuNPs/SPCE showed an unnoticeable peak. Upon modification with TC4, bands started appearing at 3360.56 cm^{-1} , indicating O–H stretching, whereas bands appearing at 2954.46 cm^{-1} and 2903.53 cm^{-1} represented C–H stretching. The bands present at 1723.75 cm^{-1} and 1421.18 cm^{-1} signified C–H bending (overtone) and O–H bending, respectively. A weaker band intensity was observed for the TC4-modified electrode as compared to the TC4 compound because of TC4's low concentration on AuNPs/SPCE.

3.1.2. Field Emission Scanning Electron Microscopy and Energy Dispersive X-ray

Figure 2 shows the surface morphologies of the modified electrode analysed via FESEM. It can be seen that the surface morphologies changed as a result of the different modification step. The bare screen-printed carbon electrode (Figure 2a) showed a densely packed rough surface, with no signs of holes on the surface layer, which is consistent with previous literature [36]. Once the gold was electrodeposited on SPCE, cauliflower-shaped particles were observed—dispersed homogeneously on the surface of the carbon working electrode, as shown in Figure 2b. These cauliflower-shaped particles may be due to the agglomeration of the electrodeposited gold nanoparticles. The modification of AuNPs/SPCE with TC4 shows a similar image but rougher surface (Figure 2c). This result may be due to the size of TC4 compound, which is small and difficult to observe because of the rough carbon background.

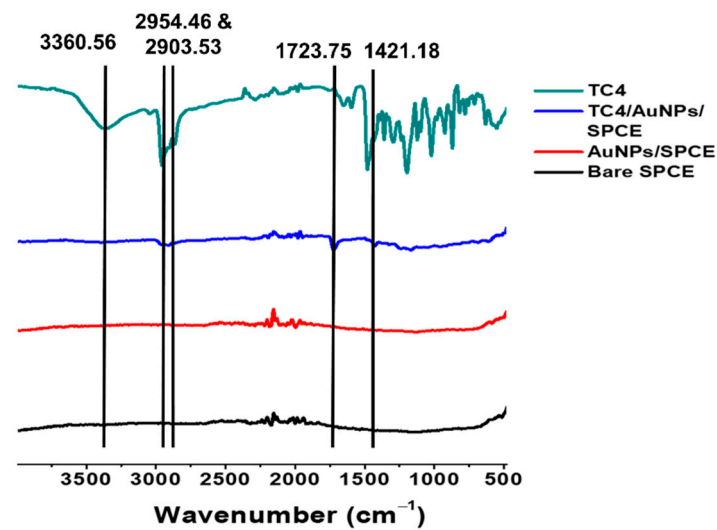


Figure 1. The FTIR spectra of the bare screen-printed carbon electrode (SPCE), gold nanoparticles/screen-printed carbon electrode (AuNPs/SPCE), thiolated calix[4]arene/gold nanoparticles/screen-printed carbon electrode (TC4/AuNPs/SPCE), and TC4 solid compound.

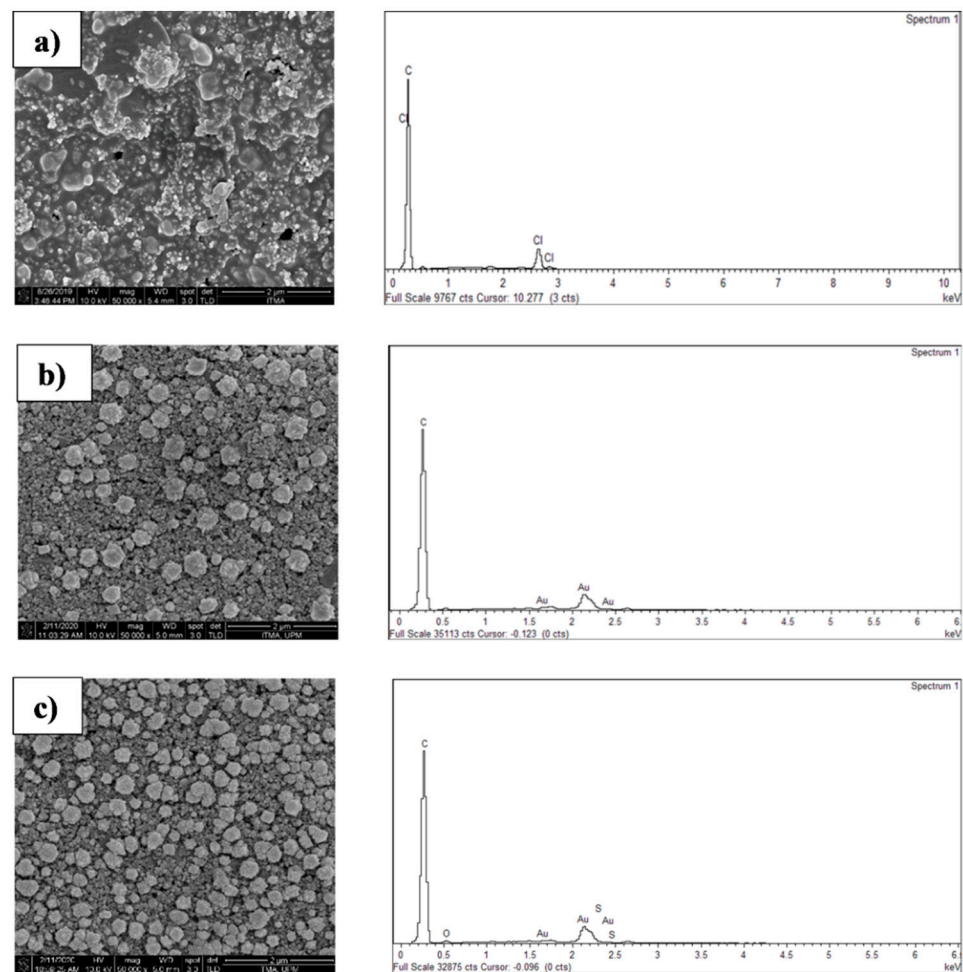


Figure 2. FESEM images and EDX graphs of (a) bare screen-printed carbon electrode (SPCE), (b) AuNPs/SPCE, and (c) TC4/AuNPs/SPCE.

Elemental composition analysis was further conducted using energy dispersive X-ray analysis. Figure 2 also shows the EDX graph and Table S1 shows the element analysis of

bare SPCE, AuNPs/SPCE, and TC4/AuNPs/SPCE. Elements C and Au presented after the carbon working electrode was modified with gold nanoparticles, whereas elements C, O, S, and Au presented after TC4 was modified on AuNPs/SPCE. Hence, it can be concluded that TC4 successfully modified on AuNPs/SPCE.

3.1.3. Electrochemical Behaviour of the Modified Electrode

The electrochemical characteristics of the modified electrodes were investigated via cyclic voltammetry in a solution containing 1 mM of a $K_3[Fe(CN)_6]$ redox probe and 0.1 M of KCl solution. Figure 3 shows the cyclic voltammograms of the bare SPCE, AuNPs/SPCE, and TC4/AuNPs/SPCE. A pair of reversible redox peaks in the cyclic voltammogram were observed, ascribed to the one-electron electrochemical process of $Fe(CN)_6^{3-/4-}$ [37]. The modification of SPCE with AuNPs improved the redox peak current, attributed to the conductive properties of AuNPs. However, the peak current decreased slightly after AuNPs/SPCE was modified with TC4. This is because TC4 on the AuNPs/SPCE surface could not recognise anions, and thus blocked the electron transfer between $Fe(CN)_6^{3-/4-}$ and the electrode surface [37]. The behaviour of the modified electrodes was further supported by the EIS data (Figure S1). The impedance data was analysed via the Randles circuit (insert of Figure S1), consisting of the solution resistance (R_s), the charge transfer resistance (R_{ct}), the Warburg, and the double-layer capacitance (C_{dl}). The resistances for the bare SPCE, the AuNPs/SPCE, and the TC4/AuNPs/SPCE were 89.2 k Ω , 28.3 k Ω , and 47.9 k Ω , respectively. The AuNPs/SPCE possessed the lowest resistance because of its significantly large specific surface area and the inherent excellent conductivity of the gold nanoparticles that promoted the electron transfer and mass exchange of electroactive species on the film surface [35]. Nevertheless, further modification of TC4 on the AuNPs/SPCE surface led to increased resistance, attributed to the nonconducting property of thiolated calix[4]arene.

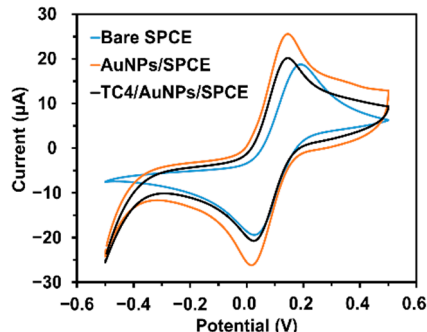


Figure 3. Cyclic voltammograms of bare SPCE, AuNPs/SPCE, and TC4/AuNPs/SPCE in 0.1 M KCl solution containing 1 mM of $K_3[Fe(CN)_6]$ at a scan rate of 100 mV/s.

3.2. Optimization Study

This study optimized the various voltammetric parameters, such as pH, deposition potential, and deposition time, to obtain the maximum current response and low detection limits. Figure 4a shows the peak current response of TC4/AuNPs/SPCE in Pb^{2+} and Cu^{2+} from pH 5 to pH 9. When the pH increased, the peak signals of Pb^{2+} and Cu^{2+} increased until pH 8. The stripping signals then gradually decreased upon reaching pH 9. The pH values below pH 5 were not considered in this study due to the competitive ligand binding in the TC4 cavity between hydrogen ions and the positively charged analytes [38]. Hence, there would be lesser concentrations of Pb^{2+} and Cu^{2+} adsorbed onto the surface. As the pH increases, the deprotonation of the $-OH$ group in the lower rim of TC4 will generate phenoxide anions, which tend to form complexes with Pb^{2+} and Cu^{2+} . However, the high pH value caused the metal ions to hydrolyse; hence, the metal ions precipitated as hydroxides [17,39].



where, M = Pb or Cu [40].

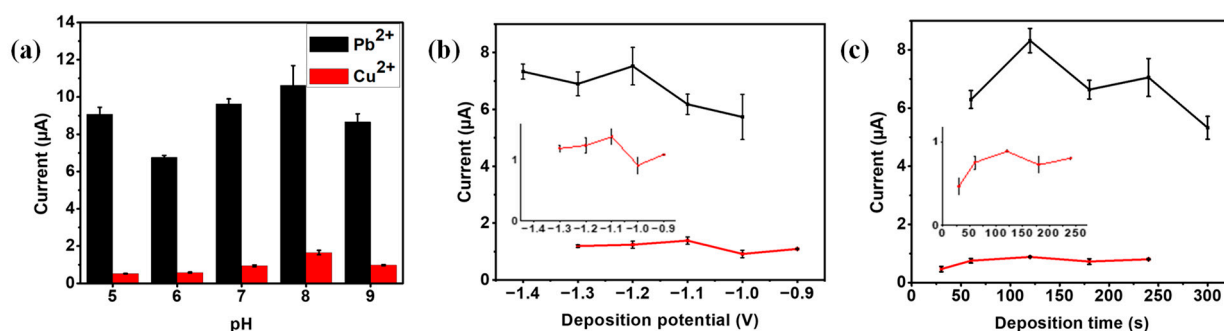


Figure 4. Current response of TC4/AuNPs/SPCE in detecting 1.0 ppm Pb^{2+} and Cu^{2+} in 0.1 M KCl solution with different (a) pH levels with a constant deposition potential of -1.2 V and a deposition time of 120 s; (b) deposition potential with a constant deposition time of 120 s in pH 8, 0.1 M KCl solution; (c) deposition time with a constant deposition potential of -1.2 V (Pb^{2+}) and -1.1 V (Cu^{2+}) in pH 8, 0.1 M KCl solution using differential pulse voltammetry (DPV).

The effect of the deposition potential on the current responses of Pb^{2+} and Cu^{2+} was studied in the range of -1.4 V to -1.0 V and -1.3 V to -0.9 V, respectively (Figure 4b). The peak currents increased when the potential was varied from -1.0 V to -1.2 V (Pb^{2+}) and from -0.9 V to -1.1 V (Cu^{2+}). The maximum peaks were achieved at -1.2 V and -1.1 V to detect Pb^{2+} and Cu^{2+} , respectively. However, a deposition potential more negative than -1.2 V and -1.1 V led to a decrease in the peak current attributed to hydrogen evolution [41]. Therefore, -1.2 V and -1.1 V are the optimal deposition potentials for detecting Pb^{2+} and Cu^{2+} .

Figure 4c shows the stripping current value of Pb^{2+} and Cu^{2+} as the accumulation time varied. The increased current response from 60 s to 120 s and 30 s to 120 s, respectively, is attributed to the increased respective amount of Pb^{2+} and Cu^{2+} on the modified electrode surface. After 120 s, a plateau was observed. The peak current was found to decrease after 120 s because of the surface saturation of the modified electrode [16]. Hence, 120 s was selected as the optimal accumulation time for Pb^{2+} and Cu^{2+} .

3.3. Mechanism of Detection

Under optimal conditions, the stripping current of bare SPCE, AuNPs/SPCE, and TC4/AuNPs/SPCE toward 1.0 ppm analytes was compared and the results presented in Figure 5. The current for detecting Pb^{2+} and Cu^{2+} using TC4/AuNPs/SPCE was higher than that of the bare SPCE and AuNPs/SPCE. Hence, TC4/AuNPs/SPCE is favourable for both Pb^{2+} and Cu^{2+} detection. For the interaction mechanism, the hydroxyl groups (as the electron donor) located at the lower rim of TC4 are the potential elements for coordinating Pb^{2+} and Cu^{2+} ions (electron acceptor) through electrostatic interaction that help induce complex formation (Figure 6).

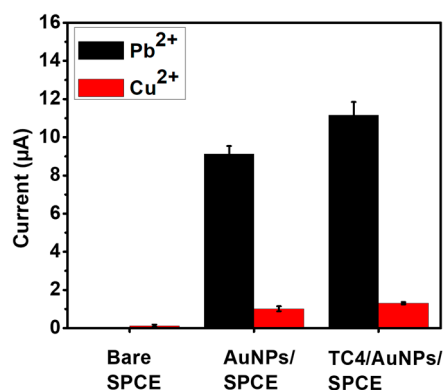


Figure 5. Comparison of 1.0 ppm Pb^{2+} and Cu^{2+} detection using bare SPCE, AuNPs/SPCE, and TC4/AuNPs/SPCE in 0.1 M, pH 8 KCl at optimum conditions of 120 s deposition time and a deposition potential of -1.2 V (Pb^{2+}) and -1.1 V (Cu^{2+}).

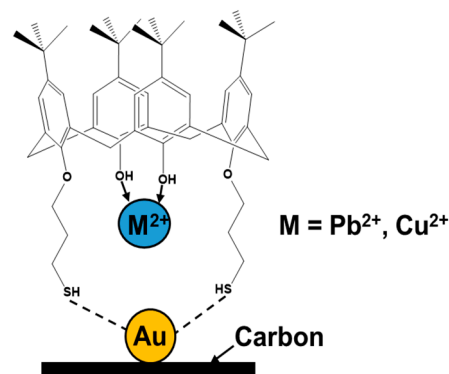


Figure 6. Schematic representation of the binding and complexation mode of TC4/AuNPs/SPCE with Pb^{2+} and Cu^{2+} .

3.4. Detection of Pb^{2+} and Cu^{2+}

The DPV responses of TC4/AuNPs/SPCE toward different concentration of Pb^{2+} and Cu^{2+} were recorded under optimal experimental conditions (Figure 7). Based on Figure 7a,c, the current response increased proportionally with increased Pb^{2+} and Cu^{2+} concentrations from 0.2 ppm to 1.0 ppm. The calibration plots (as shown in Figure 7b,d presented as straight-line graphs with a good linear regression coefficient of 0.9714 (Pb^{2+}) and 0.9926 (Cu^{2+}). The limit of detection (LOD) was calculated based on the formula $3\sigma/S$, where σ is the standard deviation of the blank and “S” is the slope of the calibration plot [14]. The LOD for Pb^{2+} and Cu^{2+} was 0.7982×10^{-2} ppm and 1.3358×10^{-2} ppm, respectively, which is beyond the permissible level set by the World Health Organization (WHO), at 0.01 ppm (Pb^{2+}) and 1.0 ppm (Cu^{2+}). Table 1 shows the performance of recently developed sensors of Pb^{2+} and Cu^{2+} as compared to the proposed sensor, TC4/AuNPs/SPCE. According to the tabulated data, the developed electrochemical sensor, is reliably used for Pb^{2+} and Cu^{2+} detection as the LOD values achieved were lower than the permissible level.

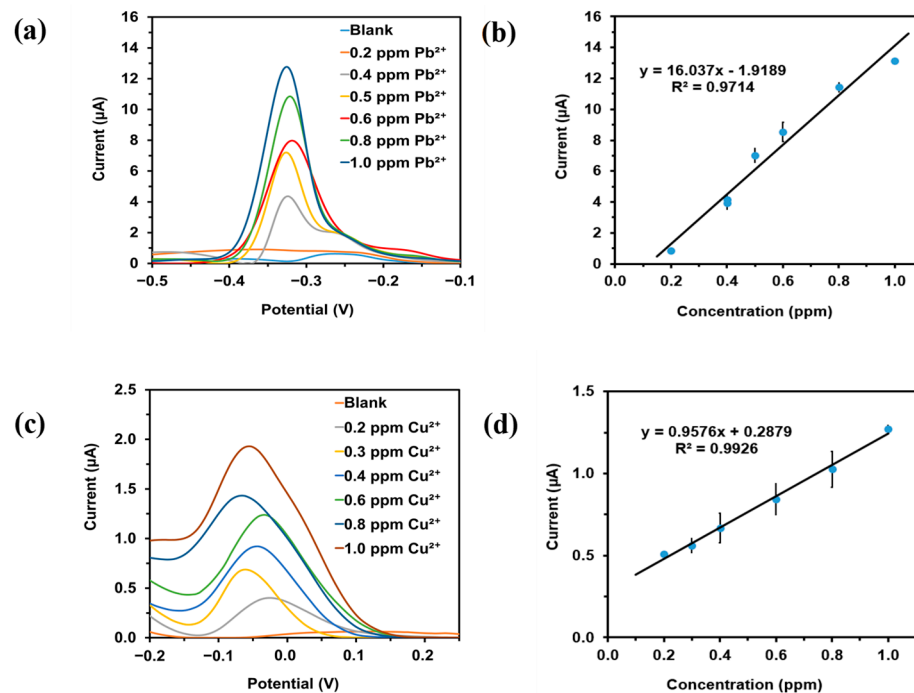


Figure 7. The DPV response of the TC4/AuNPs/SPCE toward (a) lead ions (Pb^{2+}) and (c) copper ions (Cu^{2+}). The calibration curve of (b) lead ions (Pb^{2+}) and (d) copper ions (Cu^{2+}).

Table 1. Comparison of the performance of recently developed sensors and the proposed sensor toward Pb^{2+} and Cu^{2+} .

Analytes	Electrode	Detection Range	Limitation of Detection (LOD)	Reference
Pb^{2+}	Double-walled carbon nanotubes (DWCNTs) noncovalently functionalised with <i>Allium sativum</i> extract on GCEs on GCE	0.50×10^{-2} – 10.00×10^{-2} ppm *	0.15×10^{-2} ppm *	[42]
	Polypyrrole nanoparticles on GCE	2.07×10^{-2} – 1036.00×10^{-2} ppm *	1.14×10^{-2} ppm *	[43]
	Carbon graphite powder with $\text{Na}_2\text{Mn}_2\text{Cr}(\text{PO}_4)_3$ on carbonpaste electrode	4.14×10^{-2} – 2072.00×10^{-2} ppm *	5.18×10^{-2} ppm *	[44]
	MWCNTs-COOH/UiO-66-NH ₂ /MWCNTs-COOH/GCE) on GCE	0.10×10^{-2} – 12.1×10^{-2} ppm *	0.07×10^{-3} ppm *	[45]
Cu^{2+}	TC4/AuNPs/SPCE	0.20 ppm–1.00 ppm	0.80×10^{-2} ppm	This work
	Polypyrrole-modified electrode	0.06×10^{-4} – 6355.00×10^{-2} ppm *	0.01×10^{-2} ppm *	[46]
	OP30–2.0-CSs/GCE-modified electrode	3.18×10^{-2} – 31.78×10^{-2} ppm *	0.06×10^{-2} ppm *	[47]
	HNQP/SPCE	0.00×10^{-2} – 635.50×10^{-2} ppm *	0.90×10^{-2} ppm *	[48]
	GCE/MWCNTs-BCS	3.17×10^{-2} – 38.13×10^{-2} ppm *	0.95×10^{-2} ppm *	[49]
	TC4/AuNPs/SPCE	0.20 ppm–1.00 ppm	1.34×10^{-2} ppm	This work

* The unit is converted to ppm for comparison purposes.

It is important to determine the selectivity of TC4/AuNPs/SPCE in the presence of competitor metal ions so the performance of the developed sensor can be evaluated. Hence, an interference study was carried out in the presence of 1.0 ppm of competitive ions, namely lead (Pb^{2+}), cadmium (Cd^{2+}), magnesium (Mg^{2+}), nickel (Ni^{2+}), calcium (Ca^{2+}), copper (Cu^{2+}), zinc (Zn^{2+}), and mercury (Hg^{2+}) ions. Table 2 shows no significant changes in current response when detecting Pb^{2+} except in the presence of the Zn^{2+} and Hg^{2+} competitive ions. For lead ion detection, most interferent ions had little interference on the current response of detection, possibly owing to the sensor interface possessing more selectivity/specificity toward lead ions [17]. However, the presence of interferent ions in Cu^{2+} ion detection significantly affected the current response, except for Ca^{2+} and Mg^{2+} . This result may be ascribed to the formation of intermetallic compounds between Ni^{2+} , Zn^{2+} , Cd^{2+} , Hg^{2+} , Pb^{2+} , and Cu^{2+} deposited onto the electrode interface [17,50]. Therefore, it would be worth exploring further the addition a shelter reagent in the presence of interferents, as proposed in previous literature [51].

3.5. Reproducibility, Stability, and Lifetime Studies

The reproducibility of the proposed electrode was carried out using five different modified electrodes to detect 1.0 ppm of analytes (Pb^{2+} or Cu^{2+}), while the stability study was performed by conducting five-time repetitive measurements on the target analytes using a single modified electrode. Table 3 shows excellent reproducibility and stability with good relative standard deviation (RSD) values of 3.08% and 3.59% for Pb^{2+} and Cu^{2+} , respectively. The RSD was <6.61% after five repetition runs for both target molecules.

The lifetime of the modified electrode was studied to monitor the efficiency of the electrochemical sensor in sensing target analytes (Pb^{2+} and Cu^{2+}) after a set amount of storage time. The storage durations for this study were set to 0, 7, 15, 22, and 31 days. At 0 days, the target analytes were detected using freshly modified electrodes. Table 4 and Figure S4 show the results with a reduction in current response in detecting Pb^{2+} and

Cu^{2+} , suggesting storage stability can last for at least less than 7 days to have reliable measurements.

Table 2. Current response of the TC4/AuNPs/SPCE sensor in the detection of 1.0 ppm Pb^{2+} and Cu^{2+} with the presence of different interferent ions at the same concentration (1.0 ppm) in 0.1 M, pH 8 KCl using the DPV procedure at a deposition potential of -1.2 V (Pb^{2+}) and -1.1 V (Cu^{2+}) and a deposition time of 120 s.

Interferent	Pb^{2+}		Cu^{2+}	
	Signal Change (%)	RSD (%)	Signal Change (%)	RSD (%)
Cd^{2+}	-4.80	5.19	81.79	13.25
Mg^{2+}	3.25	1.99	22.64	14.34
Ni^{2+}	19.37	5.30	61.67	7.57
Ca^{2+}	10.94	3.03	16.68	8.70
Zn^{2+}	36.04	3.77	70.68	5.04
Hg^{2+}	35.81	4.64	77.68	1.84
Cu^{2+}	19.23	6.30	-	-
Pb^{2+}	-	-	91.71	12.50

Table 3. Reproducibility and stability of TC4/AuNPs/SPCE for the detection of 1.0 ppm Pb^{2+} and Cu^{2+} .

Analytes	Reproducibility RSD (%)	Stability RSD (%)
Pb^{2+}	3.08	6.61
Cu^{2+}	3.59	2.12

Table 4. Lifetime measurement of TC4/AuNPs/SPCE in the detection of 1.0 ppm of Pb^{2+} and Cu^{2+} in 0.1 M, pH 8 KCl at deposition potential of -1.2 V (Pb^{2+}) and -1.1 V (Cu^{2+}), and a deposition time of 120 s.

Lifetime	Pb^{2+}		Cu^{2+}	
	Signal Change (%)	RSD	Signal Change (%)	RSD
7 days	24.98	6.06	29.03	5.43
15 days	31.55	4.26	38.42	12.69
22 days	47.99	6.77	41.30	13.70
31 days	60.25	11.36	43.39	5.71

3.6. Recovery Study

To verify the applicability of the developed sensor for the determination of Pb^{2+} and Cu^{2+} , an electrochemical analysis was performed where the concentration of analytes was recovered from river water and a standard solution, and the results were compared with a conventional standard method (ICP-OES). Both samples were spiked with 1 ppm analyte concentration. According to Table 5, the developed sensor showed satisfactory recoveries of 94.0%, and 103.0% for Pb^{2+} and Cu^{2+} , respectively, in deionised water, and 95.0% and 99.0%, respectively, in river water. The data obtained is in good agreement with the ICP-OES results, illustrating that the developed electrochemical sensor shows a good recovery from deionised water or in river water samples. The TC4/AuNPs/SPCE, therefore, has great potential for use in practical sample determination.

Table 5. Data validation of lead and copper ion detection in water samples.

Method	Samples	Added Pb(II) (ppm)	Found Pb(II) (ppm)	Recovery (%)	RSD (%)	Added Cu(II) (ppm)	Found Cu(II) (ppm)	Recovery (%)	RSD (%)
ICP-OES	Deionised water	1 ppm	0.89	89	1.15	1 ppm	1.03	103	0.35
TC4	Deionised water	1 ppm	0.94	94	0.66	1 ppm	1.03	103	2.83
TC4	Deionised water	0.6 ppm	0.64	105.94	3.26	0.6 ppm	0.58	96.67	3.42
ICP-OES	River water	1 ppm	0.98	98	2.03	1 ppm	1.08	108	0.11
TC4	River water	1 ppm	0.95	95	1.9	1 ppm	0.99	99	2.75
TC4	River water	2 ppm	2.1	108	3.05	2 ppm	1.88	94	3.47

4. Conclusions

The TC4/AuNPs/SPCE was developed and characterised using Fourier-transform infrared spectroscopy, field emission scanning electron microscopy, and electrochemical techniques. This system was successfully applied in the detection of lead ions (Pb^{2+}) and copper ions (Cu^{2+}) at select ppm levels using differential pulse voltammetry. The optimum current response was attained with pH 8.0, a deposition potential of -1.2 V (Pb^{2+}) and -1.1 V (Cu^{2+}), and a deposition time of 120 s. Under these optimum experimental conditions, a good linear relationship was achieved in the concentration study, ranging from 0.2 ppm to 1.0 ppm. The sensor displayed good reproducibility with an RSD of 3.08%, and 3.59% for lead ions (Pb^{2+}) and copper ions (Cu^{2+}), respectively. Most importantly, this innovative electrochemical sensor was successfully applied in detecting lead ions (Pb^{2+}) and copper (Cu^{2+}) ions in a real water sample, that is river water. However, it can be employed as an alternative sensing platform for lead ion (Pb^{2+}) determination in various sample matrices as TC4/AuNPs/SPCE is prone to detect Pb^{2+} ions rather than copper (Cu^{2+}) ions without significant interfere from competitive metal ions.

Supplementary Materials: The following are available online at <https://www.mdpi.com/article/10.3390/chemosensors9070157/s1>, Table S1: element analysis of (a) bare screen-printed carbon electrode (SPCE) (b) AuNPs/SPCE and (c) TC4/AuNPs/SPCE; Figure S1: Graph of Nyquist plot of bare SPCE, AuNPs/SPCE, TC4/AuNPs/SPCE in 0.1 M KCl containing 1.0 mM $\text{K}_3[\text{Fe}(\text{CN})_6]$ from 100 kHz to 0.1 Hz, 10 per decade and 0.005 V amplitude; Figure S2: Reproducibility of TC4/AuNPs/SPCE for 1.0 ppm Pb^{2+} and Cu^{2+} detection; Figure S3: Stability of TC4/AuNPs/SPCE for 1.0 ppm Pb^{2+} and Cu^{2+} detection; Figure S4: Lifetime measurement of TC4/AuNPs/SPCE in the detection of 1.0 ppm of Pb^{2+} and Cu^{2+} in 0.1 M, pH 8 KCl at deposition potential of -1.2 V (Pb^{2+}) and -1.1 V (Cu^{2+}), and a deposition time of 120 s.

Author Contributions: Conceptualization, C.J.M. and S.A.A.A.; methodology, C.J.M. and S.A.A.A.; validation, C.J.M.; investigation, C.J.M.; writing—original draft preparation, C.J.M.; writing—review and editing, S.A.A.A.; supervision, S.A.A.A. and N.A.Y. All authors have read and agreed to the published version of the manuscript.

Funding: This research was funded by the Ministry of Higher Education under reference code PRGS/1/2018/STG01/UPM/02/1.

Institutional Review Board Statement: Not applicable.

Informed Consent Statement: Not applicable.

Data Availability Statement: Not applicable.

Acknowledgments: The authors would like to thank the Ministry of Higher Education for funding this project via grant code PRGS/1/2018/STG01/UPM/02/1. The authors gratefully acknowledge

Irene Ling (Monash University Malaysia) for providing the 5,11,17,23-tetra-*tert*-butyl-25,27-bis(3-thiol-1-oxypropane)-26,28-dihydroxycalix[4]arene (TC4) for this project.

Conflicts of Interest: The authors declare no conflict of interest.

References

1. Pourret, O.; Hursthouse, A. It's time to replace the term "heavy metals" with "potentially toxic elements" when reporting environmental research. *Int. J. Environ. Res. Public Health* **2019**, *16*, 4446. [[CrossRef](#)] [[PubMed](#)]
2. Meseldzija, S.; Petrovic, J.; Onjia, A.; Volkov-Husovic, T.; Nestic, A.; Vukelic, N. Utilization of agro-industrial waste for removal of copper ions from aqueous solutions and mining-wastewater. *J. Ind. Eng. Chem.* **2019**, *75*, 246–252. [[CrossRef](#)]
3. Moreira, V.; Lebron, Y.; Freire, S.; Santos, L.; Palladino, F.; Jacob, R. Biosorption of copper ions from aqueous solution using *Chlorella pyrenoidosa*: Optimization, equilibrium and kinetics studies. *Microchem. J.* **2019**, *145*, 119–129. [[CrossRef](#)]
4. Du, T.; Wang, J.; Zhang, T.; Zhang, L.; Yang, C.; Yue, T.; Sun, J.; Li, T.; Zhou, M.; Wang, J. An Integrating Platform of Ratiometric Fluorescent Adsorbent for Unconventional Real-Time Removing and Monitoring of Copper Ions. *ACS Appl. Mater. Interfaces* **2020**, *12*, 13189–13199. [[CrossRef](#)] [[PubMed](#)]
5. Adilah, A.N.; Nadia, H.N. Water Quality Status and Heavy Metal Contains in Selected Rivers at Tasik Chini due to Increasing Land Use Activities. In Proceedings of the IOP Conference Series: Materials Science and Engineering, Borovets, Bulgaria, 26–29 November 2020.
6. Rehman, K.; Fatima, F.; Waheed, I.; Akash, M.S.H. Prevalence of exposure of heavy metals and their impact on health consequences. *J. Cell. Biochem.* **2018**, *119*, 157–184. [[CrossRef](#)]
7. Rane, S.J.; Sivaraman, G.; Pushpalatha, A.M.; Muthusubramanian, S. Quinoline based sensors for bivalent copper ions in living cells. *Sens. Actuators B Chem.* **2018**, *255*, 630–637. [[CrossRef](#)]
8. Liu, Y.; Ding, D.; Zhen, Y.; Guo, R. Amino acid-mediated 'turn-off/turn-on' nanozyme activity of gold nanoclusters for sensitive and selective detection of copper ions and histidine. *Biosens. Bioelectron.* **2017**, *92*, 140–146. [[CrossRef](#)]
9. Mahdi, Z.; Yu, Q.J.; El Hanandeh, A. Investigation of the kinetics and mechanisms of nickel and copper ions adsorption from aqueous solutions by date seed derived biochar. *J. Environ. Chem. Eng.* **2018**, *6*, 1171–1181. [[CrossRef](#)]
10. Tsade, H.K. Atomic absorption spectroscopic determination of heavy metal concentrations in Kulufo River, Arbaminch, Gamo Gofa, Ethiopia. *J. Environ. Anal. Chem.* **2016**, *3*, 1–3.
11. Yarur, F.; Macairan, J.-R.; Naccache, R. Ratiometric detection of heavy metal ions using fluorescent carbon dots. *Environ. Sci. Nano* **2019**, *6*, 1121–1130. [[CrossRef](#)]
12. Alkas, F.B.; Shaban, J.A.; Sukuroglu, A.A.; Kurt, M.A.; Battal, D.; Saygi, S. Monitoring and assessment of heavy metal/metalloid concentration by inductively coupled plasma mass spectroscopy (ICP-MS) method in Gonyeli Lake, Cyprus. *Environ. Monit. Assess.* **2017**, *189*, 1–8. [[CrossRef](#)]
13. Erdemir, S.; Malkondu, S. Calix[4]arene based a NIR-fluorescent sensor with an enhanced Stokes shift for the real-time visualization of Zn(II) in living cells. *Sens. Actuators B Chem.* **2020**, *306*, 127574. [[CrossRef](#)]
14. Aziz, S.F.N.A.; Zawawi, R.; Ahmad, S.A.A. An Electrochemical Sensing Platform for the Detection of Lead Ions Based on Dicarboxyl-Calix[4]arene. *Electroanalysis* **2018**, *30*, 533–542. [[CrossRef](#)]
15. Sultan, S.; Shah, A.; Khan, B.; Qureshi, R.; Al-Mutawah, J.I.; Shah, M.R.; Shah, A.H. Simultaneous Ultrasensitive Detection of Toxic Heavy Metal Ions Using bis(imidazo[4,5-f][1,10]phenanthroline) Appended bis-triazolo Calix[4] Arene (8)/Glassy Carbon Electrode. *J. Electrochem. Soc.* **2019**, *166*, B1719. [[CrossRef](#)]
16. Adarakatti, P.S.; Foster, C.W.; Banks, C.E.; NS, A.K.; Malingappa, P. Calixarene bulk modified screen-printed electrodes (SPCCEs) as a one-shot disposable sensor for the simultaneous detection of lead(II), copper(II) and mercury(II) ions: Application to environmental samples. *Sens. Actuators A Phys.* **2017**, *267*, 517–525. [[CrossRef](#)]
17. Adarakatti, P.S.; Siddaramanna, A.; Malingappa, P. Fabrication of a new calix[4]arene-functionalized Mn₃O₄ nanoparticle-based modified glassy carbon electrode as a fast responding sensor towards Pb²⁺ and Cd²⁺ ions. *Anal. Methods* **2019**, *11*, 813–820. [[CrossRef](#)]
18. Rana, S.; Mittal, S.K.; Singh, N.; Singh, J.; Banks, C.E. Schiff base modified screen printed electrode for selective determination of aluminium(III) at trace level. *Sens. Actuators B Chem.* **2017**, *239*, 17–27. [[CrossRef](#)]
19. Metters, J.P.; Kadara, R.O.; Banks, C.E. New directions in screen printed electroanalytical sensors: An overview of recent developments. *Analyst* **2011**, *136*, 1067–1076. [[CrossRef](#)] [[PubMed](#)]
20. Hwang, J.-H.; Wang, X.; Zhao, D.; Rex, M.M.; Cho, H.J.; Lee, W.H. A novel nanoporous bismuth electrode sensor for in situ heavy metal detection. *Electrochim. Acta* **2019**, *298*, 440–448. [[CrossRef](#)]
21. Lee, S.; Oh, J.; Kim, D.; Piao, Y. A sensitive electrochemical sensor using an iron oxide/graphene composite for the simultaneous detection of heavy metal ions. *Talanta* **2016**, *160*, 528–536. [[CrossRef](#)]
22. Silwana, B.; van der Horst, C.; Iwuoha, E.; Somerset, V. Screen-printed carbon electrodes modified with a bismuth film for stripping voltammetric analysis of platinum group metals in environmental samples. *Electrochim. Acta* **2014**, *128*, 119–127. [[CrossRef](#)]
23. Durai, L.; Badhulika, S. Ultra-selective, trace level detection of As³⁺ ions in blood samples using PANI coated BiVO₄ modified SPCE via differential pulse anode stripping voltammetry. *Mater. Sci. Eng. C* **2020**, *111*, 110806. [[CrossRef](#)]

24. Wu, K.-H.; Lo, H.-M.; Wang, J.-C.; Yu, S.-Y.; Yan, B.-D. Electrochemical detection of heavy metal pollutant using crosslinked chitosan/carbon nanotubes thin film electrodes. *Mater. Express* **2017**, *7*, 15–24. [[CrossRef](#)]
25. Pudza, M.Y.; Abidin, Z.Z.; Abdul-Rashid, S.; Yasin, F.M.; Noor, A.S.M.; Abdullah, J. Selective and simultaneous detection of cadmium, lead and copper by tapioca-derived carbon dot-modified electrode. *Environ. Sci. Pollut. Res.* **2020**, *27*, 1–10. [[CrossRef](#)]
26. Jian, J.-M.; Liu, Y.-Y.; Zhang, Y.-L.; Guo, X.-S.; Cai, Q. Fast and sensitive detection of Pb²⁺ in foods using disposable screen-printed electrode modified by reduced graphene oxide. *Sensors* **2013**, *13*, 13063–13075. [[CrossRef](#)] [[PubMed](#)]
27. Cui, L.; Wu, J.; Ju, H. Label-free signal-on aptasensor for sensitive electrochemical detection of arsenite. *Biosens. Bioelectron.* **2016**, *79*, 861–865. [[CrossRef](#)]
28. Chen, Y.; Zheng, G.; Shi, Q.; Zhao, R.; Chen, M. Preparation of thiolated calix[8]arene/AuNPs/MWCNTs modified glassy carbon electrode and its electrocatalytic oxidation toward paracetamol. *Sens. Actuators B Chem.* **2018**, *277*, 289–296. [[CrossRef](#)]
29. Wang, L.; Wang, X.; Shi, G.; Peng, C.; Ding, Y. Thiacalixarene Covalently Functionalized Multiwalled Carbon Nanotubes as Chemically Modified Electrode Material for Detection of Ultratrace Pb²⁺ Ions. *Anal. Chem.* **2012**, *84*, 10560–10567. [[CrossRef](#)] [[PubMed](#)]
30. Pulkkinen, P.M.S.; Hassinen, J.; Ras, R.; Tenhu, H. Gold nanoparticles: Calixarene complexation in a mixed calixarene–alkanethiol monolayer. *RSC Adv.* **2014**, *4*, 13453–13460. [[CrossRef](#)]
31. Pereira, S.V.; Bertolino, F.; Fernández-Baldo, M.A.; Messina, G.A.; Salinas, E.; Sanz, M.I.; Raba, J. A microfluidic device based on a screen-printed carbon electrode with electrodeposited gold nanoparticles for the detection of IgG anti-Trypanosoma cruzi antibodies. *Analyst* **2011**, *136*, 4745–4751. [[CrossRef](#)]
32. Dechtrirat, D.; Yingyuad, P.; Prajongtat, P.; Chuenchom, L.; Sriprachubwong, C.; Tuantranont, A.; Tang, I.-M. A screen-printed carbon electrode modified with gold nanoparticles, poly (3,4-ethylenedioxythiophene), poly (styrene sulfonate) and a molecular imprint for voltammetric determination of nitrofurantoin. *Microchim. Acta* **2018**, *185*, 1–9. [[CrossRef](#)] [[PubMed](#)]
33. Guo, S.; Wang, E. Synthesis and electrochemical applications of gold nanoparticles. *Anal. Chim. Acta* **2007**, *598*, 181–192. [[CrossRef](#)] [[PubMed](#)]
34. Zainal, P.N.S.; Ahmad, S.A.A.; Ngee, L.H.; Ling, I. Development of Electrochemical Sensor Based on Thiolated Calixarene-Functionalized Gold Nanoparticles for the Selective Recognition of Anthracene. *IEEE Sens. J.* **2020**, *21*, 5703–5710. [[CrossRef](#)]
35. Lu, Z.; Zhang, J.; Dai, W.; Lin, X.; Ye, J.; Ye, J. A screen-printed carbon electrode modified with a bismuth film and gold nanoparticles for simultaneous stripping voltammetric determination of Zn(II), Pb(II) and Cu(II). *Microchim. Acta* **2017**, *184*, 4731–4740. [[CrossRef](#)]
36. Obaje, E.A.; Cummins, G.; Schulze, H.; Mahmood, S.; Desmulliez, M.P.; Bachmann, T.T. Carbon screen-printed electrodes on ceramic substrates for label-free molecular detection of antibiotic resistance. *J. Interdiscip. Nanomed.* **2016**, *1*, 93–109. [[CrossRef](#)]
37. Zheng, G.; Chen, M.; Liu, X.; Zhou, J.; Xie, J.; Diao, G. Self-assembled thiolated calix[n]arene (n = 4, 6, 8) films on gold electrodes and application for electrochemical determination dopamine. *Electrochim. Acta* **2014**, *136*, 301–309. [[CrossRef](#)]
38. Liu, L.; Zhang, K.; Wei, Y. A simple strategy for the detection of Cu(ii), Cd(ii) and Pb(ii) in water by a voltammetric sensor on a TC4A modified electrode. *New J. Chem.* **2019**, *43*, 1544–1550. [[CrossRef](#)]
39. Adarakatti, P.S.; Malingappa, P. Amino-calixarene-modified graphitic carbon as a novel electrochemical interface for simultaneous measurement of lead and cadmium ions at picomolar level. *J. Solid State Electrochem.* **2016**, *20*, 3349–3358. [[CrossRef](#)]
40. Alva, S.; Widinugroho, A.; Adrian, M.; Khaerudini, D.S.; Pratiwi, S.E.; Aziz, A.S.A. The New Lead(II) Ion Selective Electrode Based On Free Plasticizer Film of pTHFA Photopolymer. *J. Electrochem. Soc.* **2019**, *166*, B1513. [[CrossRef](#)]
41. Pizarro, J.; Flores, E.; Jimenez, V.; Maldonado, T.; Saitz, C.; Vega, A.; Godoy, F.; Segura, R. Synthesis and characterization of the first cyrhetrenyl-appended calix[4]arene macrocycle and its application as an electrochemical sensor for the determination of Cu(II) in bivalve mollusks using square wave anodic stripping voltammetry. *Sens. Actuators B Chem.* **2019**, *281*, 115–122. [[CrossRef](#)]
42. Perrachione, F.; Dalmasso, P.R.; Gutierrez, F.A.; Rivas, G.A. Double-walled carbon nanotubes functionalized with Allium sativum (garlic extract): Analytical applications for Pb(II) electrochemical sensing. *Microchem. J.* **2021**, *160*, 105653. [[CrossRef](#)]
43. Xu, T.; Dai, H.; Jin, Y. Electrochemical sensing of lead(II) by differential pulse voltammetry using conductive polypyrrole nanoparticles. *Microchim. Acta* **2020**, *187*, 1–7. [[CrossRef](#)]
44. Benhsina, E.; Hermouche, L.; Assani, A.; Saadi, M.; Labjar, N.; El Hajjaji, S.; Lahmar, A.; El Ammari, L. Synthesis, characterization, magnetic properties, and lead sensing based on a new alluaudite-like phosphate Na₂Mn₂Cr(PO₄)₃. *J. Mater. Sci.* **2021**, *56*, 2163–2175. [[CrossRef](#)]
45. Lu, Z.; Zhao, W.; Wu, L.; He, J.; Dai, W.; Zhou, C.; Du, H.; Ye, J. Tunable electrochemical of electrosynthesized layer-by-layer multilayer films based on multi-walled carbon nanotubes and metal-organic framework as high-performance electrochemical sensor for simultaneous determination cadmium and lead. *Sens. Actuators B Chem.* **2021**, *326*, 128957. [[CrossRef](#)]
46. Bagheri, A.; Marand, M.H. Voltammetric and Potentiometric Determination of Cu²⁺ Using an Overoxidized Polypyrrole Based Electrochemical Sensor. *Russ. J. Electrochem.* **2020**, *56*, 453–461. [[CrossRef](#)]
47. Xiong, W.; Zhang, P.; Liu, S.; Lv, Y.; Zhang, D. Catalyst-free synthesis of phenolic-resin-based carbon nanospheres for simultaneous electrochemical detection of Cu(II) and Hg(II). *Diam. Relat. Mater.* **2021**, *111*, 108170. [[CrossRef](#)]
48. Maddipatla, D.; Saeed, T.S.; Narakathu, B.B.; Obare, S.O.; Atashbar, M.Z. Incorporating a Novel Hexaazatriphenylene Derivative to a Flexible Screen-Printed Electrochemical Sensor for Copper Ion Detection in Water Samples. *IEEE Sens. J.* **2020**, *20*, 12582–12591. [[CrossRef](#)]

49. Saldaña, J.; Gallay, P.; Gutierrez, S.; Eguílaz, M.; Rivas, G. Multi-walled carbon nanotubes functionalized with bathocuproinedisulfonic acid: Analytical applications for the quantification of Cu(II). *Anal. Bioanal. Chem.* **2020**, *412*, 5089–5096. [[CrossRef](#)]
50. Kokkinos, C.; Economou, A.; Raptis, I.; Efstathiou, C.E. Lithographically fabricated disposable bismuth-film electrodes for the trace determination of Pb(II) and Cd(II) by anodic stripping voltammetry. *Electrochim. Acta* **2008**, *53*, 5294–5299. [[CrossRef](#)]
51. Wang, F.; Liu, Q.; Wu, Y.; Ye, B. Langmuir–Blodgett film of p-tert-butylthiacalix[4]arene modified glassy carbon electrode as voltammetric sensor for the determination of Ag⁺. *J. Electroanal. Chem.* **2009**, *1*, 49–54. [[CrossRef](#)]